Acute and subacute pulmonary toxicity and mortality in mice after intratracheal instillation of ZnO nanoparticles in three laboratories

Jacobsen, Nicklas Raun; Stoeger, Tobias; van den Brule, Sybille; Saber, Anne Thoustrup; Beyerle, Andrea; Vietti, Giulia; Mortensen, Alicja; Szarek, Józef; Budtz, Hans Christian; Kermanizadeh, Ali; Banerjee, Atrayee; Ercal, Nuran; Vogel, Ulla Birgitte; Wallin, Håkan; Møller, Peter

Published in:
Food and Chemical Toxicology

Link to article, DOI:
10.1016/j.fct.2015.08.008

Publication date:
2015

Document Version
Publisher's PDF, also known as Version of record

Food and Chemical Toxicology 85 (2015) 84–95

Contents lists available at ScienceDirect

Food and Chemical Toxicology

journal homepage: www.elsevier.com/locate/foodchemtox

Acute and subacute pulmonary toxicity and mortality in mice after intratracheal instillation of ZnO nanoparticles in three laboratories

Nicklas Raun Jacobsen [a, *], Tobias Stoeger [b], Sybille van den Brule [c], Anne Thoustrup Saber [a], Andrea Beyerle [b], Giulia Vietti [c], Alicja Mortensen [d], Józef Szarek [e], Hans Christian Budtz [a], Ali Kermanizadeh [f], Atrayee Banerjee [g], Nuran Ercal [g], Ulla Vogel [a, h], Håkan Wallin [a, f], Peter Møller [f]

[a] National Research Centre for the Working Environment, Lersø Parkallé 105, DK, 2100 Copenhagen Ø, Denmark
[b] Institute of Lung Biology and Disease, Comprehensive Pneumology Center Helmholtz Zentrum München, German Research Center for Environmental Health, Munich, Germany
[c] Louvain Centre for Toxicology and Applied Pharmacology, Université catholique de Louvain, Avenue E. Mounier 52 – bte B1.52.12, 1200 Brussels, Belgium
[d] National Food Institute, Technical University of Denmark, Søborg, Denmark
[e] Faculty of Veterinary Medicine, University of Warmia and Mazury in Olsztyn, 10-719 Olsztyn, Poland
[f] Department of Public Health, University of Copenhagen, DK, 1014 Copenhagen K, Denmark
[g] Department of Chemistry, Missouri University of Science and Technology, Rolla, MO, USA
[h] Department of Micro- and Nanotechnology, Technical University of Denmark, DK, 2800 Lyngby, Denmark

ARTICLE INFO

Article history:
Received 2 June 2015
Received in revised form
28 July 2015
Accepted 4 August 2015
Available online 7 August 2015

Keywords:
Cytotoxicity
DNA damage
Fibrosis
Inflammation
Mortality
Oxidative stress

ABSTRACT

Inhalation is the main pathway of ZnO exposure in the occupational environment but only few studies have addressed toxic effects after pulmonary exposure to ZnO nanoparticles (NP). Here we present results from three studies of pulmonary exposure and toxicity of ZnO NP in mice. The studies were prematurely terminated because interim results unexpectedly showed severe pulmonary toxicity. High bolus doses of ZnO NP (25 up to 100 μg; ≥1.4 mg/kg) were clearly associated with a dose dependent mortality in the mice. Lower doses (≥6 μg; ≥0.3 mg/kg) elicited acute toxicity in terms of reduced weight gain, desquamation of epithelial cells with concomitantly increased barrier permeability of the alveolar/blood as well as DNA damage. Oxidative stress was shown via a strong increase in lipid peroxidation and reduced glutathione in the pulmonary tissue. Two months post-exposure revealed no obvious toxicity for 12.5 and 25 μg on a range of parameters. However, mice that survived a high dose (50 μg; 2.7 mg/kg) had an increased pulmonary collagen accumulation (fibrosis) at a similar level as a high bolus dose of crystalline silica. The recovery from these toxicological effects appeared dose-dependent. The results indicate that alveolar deposition of ZnO NP may cause significant adverse health effects.

1. Introduction

Zinc oxide (ZnO) nanoparticles (NP) are extensively used in consumer products. Worldwide production is estimated at 0.1–1.2 million tons per year (Das et al., 2011; Kumar and Dhawan, 2013). ZnO and/or ZnO NP are used in numerous products like cosmetics, sun screens, plastics, rubber, ceramics, cement, glass, paints, lubricants, electronic sensor and solar cells. Furthermore, ZnO are added to fertilizers and animal food as a source for the micronutrient (Zn) essential for hundreds of enzymes (Baxter and Aydil, 2005; Pan et al., 2001; Pinnell et al., 2000; Ma et al., 2013).

In vitro studies have shown that ZnO is cytotoxic at relatively low concentrations as compared to other types of engineered nanomaterials such as titanium dioxide, carbon nanotubes (Danielsen et al., 2014; Kermanizadeh et al., 2012, 2013a; Karlsson et al., 2014). Similar findings on cytotoxicity have been observed in broncho-alveolar lavage cells after pulmonary exposure to ZnO NP, which has been attributed to the dissolution of Zn ions (Cho et al., 2011; Kao et al., 2012). It has been shown that nanosized (50–70 nm) and fine (<1000 nm) ZnO particles elicited pulmonary inflammation and cytotoxicity in rats after inhalation and intratracheal exposure (Sayes et al., 2007; Warheit et al., 2009). Another

* Corresponding author.
E-mail address: nrj@nrcwe.dk (N.R. Jacobsen).

http://dx.doi.org/10.1016/j.fct.2015.08.008

study has shown that ZnO particles with primary sizes of 35 and 250 nm elicited a similar extent of pulmonary inflammation and cytotoxicity in Sprague–Dawley rats 24 h after a 6-hr inhalation exposure (Ho et al., 2011). The available results suggest that the dissolution of Zn ions is important for ZnO-mediated toxicity and cell death (Landsiedel et al., 2014).

ZnO NP may be expected to be more toxic than larger ZnO particles for several reasons; NP have a higher alveolar deposition leading to prolonged retention. They can escape the lung and enter the blood or lymphatic circulation. Their larger surface to mass ratio of NP should lead to faster dissolution of ZnO NP compared to larger bulk sized ZnO particles. Moreover, whereas the uptake of particles larger than 500 nm is restricted to specialized phagocytes, NPs are also effectively absorbed by the ubiquitous endocytosis pathway. By this way internalized NPs will enter the endo-lysosomal route, where in consequence of the local acid environment, the intracellular release of ions can significantly be enhanced leading to the important pathway of toxicity described as "lysosome-enhanced Trojan horse effect" (Sabella et al., 2014).

Here we present three different studies on pulmonary exposure to ZnO NP in mice. The investigations were conducted in different laboratories, using different ZnO nanomaterials and different mouse strains exposed via a fairly similar pulmonary exposure technique (instillation or aspiration). These studies were prematurely terminated because the highest exposures were unexpectedly associated with severe toxicity or death. The purpose of the present communication is to expand information on toxicological data of ZnO nanomaterials up to acute and sub-acute effects of a larger dose range.

2. Material and methods

2.1. Study #1

2.1.1. Mice and caging conditions

Female wild-type C57BL/6JBomTac (C57) mice aged 5–6 weeks were obtained from Taconic (Ry, Denmark). The mice were randomly divided into housing groups of 10 in polypropylene cages (425 mm × 266 mm × 150 mm) with pinewood sawdust bedding and enrichment in form of sticks of aspen wood and rodent tunnels (Brogaarden, Denmark). The cages were stored in rooms with a 12 h light period from 6 a.m. to 6 p.m., and the temperature and relative humidity in the animal room were 21 ± 2 °C and 50 ± 5%, respectively. The cages were sanitized on two occasions every week. All mice were given free access to tap water and standard diet (Altromin no. 1324, Altromin International, Lage, Germany). The mice were kept under conventional animal facilities and were allowed to acclimatize for 2–3 weeks before they entered the experimental protocol (Saber et al., 2012a). All mice were 8 weeks old at the time of the study, and the average weight at the day of instillation was 18 ± 1.4 g. All animal procedures followed the guidelines for the care and handling of laboratory animals according to the EC Directive 86/609/EEC and the Danish law. The Animal Experiment Inspectorate under the Danish Ministry of Justice approved the study (2012-15-2934-00223).

2.1.1.1. Nanoparticles, characterization and preparation of suspensions. The ZnO NP powder (CAS-No: 1314-13-2) (ZincoxTM 10, IBU-tec advanced materials AG, Weimar, Germany) was produced by pulsation reactor technique. According to the manufacturer the Brunauer Emmett Teller (BET) surface area was 60 ± 5 m^2/g, the spherical particles had an average size of 12 ± 3 nm and a hexagonal crystallographic phase. The purity was above 99% determined by energy dispersive x-ray analysis. Characterization of the instillation suspension by dynamic light scattering (DLS) Zetasizer nano ZS (Malvern Inc., UK.) was performed as previously described (Jacobsen et al., 2009). However, the refractive (Ri) and absorption indices (Rs) was set at 2.020 and 0.400, respectively, the values for ZnO NP. At concentrations between 0.04 and 0.36 mg/ml the ZnO NP was present in a very similar narrow and clear peak with an agglomerated number size between 59 and 68 nm. Reliable data with a low polydispersity index (PDI) (between 0.21 and 0.29) was obtained for the 3 low concentrations of ZnO NP. However, the high dose used in the pilot experiment (3.24 mg/mL; 162 μg/animal) yielded unreproducible, unreliable results likely caused by strong agglomeration, sedimentation with decreasing count rates (Zeta average size of 1–3 μm, PDI: 0.33–0.6).

The ZnO NP was suspended in 2% sibling mouse serum in MilliQ water. The suspensions were sonicated as described in Poulsen et al. (2015a) using a Branson Sonifier S-450D (Branson Ultrasonics Corp., Danbury, CT, USA) equipped with a disruptor horn (model number 101-147-037 (Jackson et al., 2011a)). Total sonication time was 16 min at an amplitude of 10%. Samples were continuously cooled on ice during the sonication procedure. For the pilot experiment a suspension of 3.24 mg/mL (162 μg/animal) was prepared. Each instillation was 50 μl suspension followed by 150 μl air. For the following study the high dose stock suspension was prepared at 0.36 mg/mL (18 μg/animal). This suspension was diluted 1:3 for the medium dose (0.12 mg/mL; 6 μg/animal) and further 1:3 for the low dose (0.04 mg/mL; 2 μg/animal). Each of these dilutions, were sonicated for 2 min. Vehicle control solutions were prepared by sonicating 2% sibling mouse serum in MilliQ water according to the full protocol.

2.1.1.2. Experimental design and exposure. Two mice were exposed in a pilot study to 162 μg ZnO NP/animal. However, on the second day these became visibly ill (immobile, pilo erection, hunched posture) and the pilot experiment was terminated following approximately 30 h. This was followed by the main study were groups of mice were given 0, 2, 6 or 18 μg ZnO NP or 162 μg carbon black Printex 90 by a single intratracheal instillation. Printex 90 is a highly inflammatory particle that has been extensively examined and used as a benchmark particle (Jacobsen et al., 2007, 2008, 2011; Jackson et al., 2012; Bourdon et al., 2012; Hogsberg et al., 2013; Vesterdal et al., 2010; Kyjovska et al., 2015a). Each exposed group consisted of six mice (N = 6) and each control group of twelve mice (N = 12) and was planned to be killed after 1d and 3d. Additionally eight unexposed mice were included in the study. A total of 80 mice were used in this study. An originally planned later time point for termination was omitted due to high toxicity. The instillation technique was performed as previously been described (Kyjovska et al., 2015b). Briefly, mice were anesthetized by inhalation of 4% isoflurane, before being placed back down on a 50° sloped instillation board. The tongue was gently pushed aside. Using an external cold light source (KL1500LED; Schott, Lyngby, Denmark), the trachea could be visualized and intubated using a 24 gauge BD Insyte catheter (Becton Dickinson, Denmark) with a shortened needle. The correct location of each intubation catheter was tested using a highly sensitive pressure transducer (pneumotachometer) developed at the National Research Centre for the Working Environment in collaboration with John Frederiksen (FFE/P, Copenhagen, Denmark). A 50 μl suspension was instilled followed by 200 μl air with a 250 μl SGE glass syringe (250F-LT-GT, MicroLab, Aarhus, Denmark). Control animals received vehicle instillations. All animals were gently downwards shaken three times to ensure that no liquids were blocking the upper respiratory airways. After instillation, the mice were weighed and transferred to the home cage until termination.

2.1.1.3. Blood, broncho-alveolar lavage fluid, cells and preparation of tissues. Mice were weighed at the day of instillation and again on the day of dissection. The mice were anesthetized using Hypnorm® (fentanyl citrate 0.315 mg/mL and fluanisone 10 mg/mL from Janssen Pharma) and Dormicum® (Midazolam 5 mg/mL from Roche). Both anesthetics were mixed with equal volumes of sterile water. A volume of 0.15 mL/25 g body weight was injected intramuscularly (half the dose per leg).

Preparation of broncho-alveolar lavage fluid (BALF) was performed as previously described (Poulsen et al., 2015b). Briefly, exsanguination was caused by withdrawal of blood from a heart puncture. BALF and cells were obtained by infusing the lungs twice with 1 mL sterile saline water per 25 g body weight. Each flush consisted of 3 slow up and downwards movements. The second flush was also performed with fresh saline water. The BALF was stored on ice until centrifuged (400 g, 4 °C, 10 min). The supernatant was divided in strips, snap-frozen in liquid-nitrogen and stored at −80 °C before quantification of protein concentration (Pierce BCA, Bie–Berntsen, Denmark) according to the manufacturer's description. The BALF cells were re-suspended in 100 μL medium (HAMF12 with 10% fetal bovine serum). The cell suspension (40 μL) was mixed with 160 μL medium containing 10% DMSO and stored at −80 °C for comet assay analysis which was performed as previously described (Saber et al., 2012b). For differential count 50 μL cell suspension was collected on a microscope slide by centrifugation at 55 g, 4 min in a Cytofuge 2 (StatSpin, Bie and Berntsen, Rødovre, Denmark). The slides were fixed with 96% EtOH and stained with May-Grünwald-Giemsa stain. The cellular composition of BALF cells was determined by scoring 200 cells. The total number of cells was determined by using the NucleoCounter (Chemometec, Allerød, Denmark) live/dead assay according to the manufacturer's instructions.

Tissue samples of liver and lung were taken from two mice in each of the three ZnO NP groups (2, 6 and 18 μg) as well as vehicle controls. The samples were fixed in neutral buffered formaldehyde (4%), trimmed, paraffin-embedded and sections of 4–6 μm were made and stained with hematoxylin and eosin for the histological examination.

2.2. Study #2

2.2.1. Mice and caging conditions

Eight to twelve weeks old, female BALB/cAnNcrl mice were obtained from Charles River Laboratories (Sulzfeld, Germany). The animals were kept in isolated ventilated cages (IVC-Racks; BioZone, Margate, UK), supplied with filtered air and a 12-hr light/12-hr dark cycle. Specific pathogen-free hygienic status was approved and certified according to the Federation of European Laboratory Animal Science Associations guidelines (Nicklas et al., 2002). Standard diet (Altromin no. 1314, Altromin International, Lage, Germany) and water were available *ad libitum*. Animals were 10–12 weeks of age with body weights between 19.6 and 23.1 g at the beginning of the study. Animal experiments were carried out according to the German law of protection of animal life and were approved by an external review committee for laboratory animal care. The approval number for the specified studies was Az55 2-1-54-2531-115-05.

2.2.1.1. Nanoparticles, preparation and characterization of suspensions. ZnO NP was obtained from Alfa Aesar (ID 43141, A Johnson Matthey Company, Karlsruhe, Germany) with a nominal average diameter of 70 nm. According to manufacturer the primary particle size is: 24–71 nm; BET surface area: 15–45 m^2/g, agglomerated. The authors have previously determined the BET size to 13 m^2/g (Lenz et al., 2013). Crystalline silica (Min-U-Sil 5, a-quartz) was obtained from U.S. Silica Company, Berkerly Springs, WV, USA, with a median diameter of 1.7 μm declared on the datasheet from the manufacturer.

ZnO NP (5 and 15 μg in 50 μl suspension) and crystalline silica (35 μg in 50ul suspension) was prepared in sterile, pyrogene-free distilled water. Stock solutions (10 mg/mL) were sonicated using a SonoPlus HD70 (Bachofer, Berlin, Germany) at a moderate energy of 20 W for 15 min prior to dilution. Each suspension was sonicated for 10 min directly before use. According to our previous experience, the instillation of 50 μL distilled water did not cause any measurable stress effects such as the expression of heat shock protein hsp70/hsp1a (Stoeger et al., 2006). Unexposed control animals were included as well as and sham exposed animals receiving 50 μL pure distilled water.

2.2.1.2. Experimental design and exposure. Controls and two dose groups (5 and 15 μg/animal) were planned to be killed 24 h, 3 days, or 7 days post-exposure. Each group consisted of 8 mice (N = 8). However, the experiment was terminated early for reasons of animal welfare (acute significant weight loss) thus only 24 h post-exposure were completed. A total of 40 mice were used for this study.

Before instillation mice were anesthetized by intraperitoneal injection of a mixture of xylazine (4.1 mg/kg body weight) and ketamine (188.3 mg/kg body weight). The animals were then fixed in a supine position on a 60° incline board by holding their upper incisor teeth. The tongue was gently extended using coated tweezers, and the mice were intubated through the mouth and trachea using a bulb headed cannula inserted 10 mm into the trachea; a suspension containing 5 or 15 μg particles, respectively, in 50 μL pyrogene-free distilled water was instilled, followed by 100 μL air.

2.2.1.3. Blood, broncho-alveolar lavage fluid and cells. Mice were weighed at the day of instillation and again on the day of dissection. They were anesthetized with an overdose of ketamine/xylazin (1%/0.1%). Exsanguination was caused by retro-orbital collection of 500–700 μl of blood. The blood was collected in EDTA-coated tubes and continuously rotated/moved prior to measurement by the ADVIA 120 Hematology System (Siemens Healthcare Diagnostics, Deerfield, USA).

The lungs of the mice were lavaged 10 times with 1 mL of fresh phosphate-buffered saline (PBS; 37 °C), supplemented with complete protease inhibitor cocktail (Roche Diagnostics, Mannheim, Germany). BALF of each animal were pooled. Cytocentrifuged slides were prepared by centrifugation (100 *g*, 5 min). BALF cells were prepared for cell differentiation with May-Grünwald staining. Two slides were prepared per animal and 2x 200 cells scored on each slide.

Total protein and lactate dehydrogenase (LDH) as well as secretion of 10 cytokines/chemokines were measured in cell-free BALF. BALF was centrifuged at 1200 g, 15 min at 4 °C. Total concentration of protein was determined using the Bradford method and LDH concentration was determined by using Cytotoxicity Detection Kit (Roche Applied Diagnostics, Germany). Levels of total IgM were measured by ELISA using complementary capture and detection antibody pairs as previously described (Beyerle et al., 2011a). Cytokine release: Ten cytokines/chemokines were detected simultaneously in the BALF using Luminex technology (Linco Research, St. Charles, MO). In this study, the secretions of the following cytokines/chemokines were investigated: Interleukin (IL)-1α, IL-6, IL-10, tumor necrosis factor (TNF)α, granulocyte-colony stimulating factor (G-CSF), chemokine (C-X-C motif) ligand (CXCL)1, CXCL-2, CXCL-5, CXCL-10, interferon (INF)γ. The assay was performed as described previously (Beyerle et al., 2011b). Monocyte chemotactic protein (MCP)-1 also called chemokine (C–C motif) ligand (CCL)2 was quantified in the BALF using mouse CCL-2/JE

DuoSet ELISA (R&D Systems, Inc., Minneapolis, USA), according to the manufacturer's instructions.

2.2.1.4. Oxidative stress parameters in lung tissue. Glutathione (GSH), malondialdehyde (MDA) levels and catalase activity in the lung tissue were determined by HPLC, as previously described (Banerjee et al., 2009).

2.3. Study #3

2.3.1. Mice and caging conditions

Eight week-old C57BL/6N female mice were obtained from Taconic Europe (Ry, Denmark). The animals were kept and housed in positive-pressure air-conditioned units (25 °C, 50% relative humidity) on a 12:12-h light/dark cycle. All mice were given free access to tap water and standard diet. The protocol of this investigation was approved by the local ethical committee for animal research. The laboratory approval number is LA1230312 and the approval for the specified studies was 2010/UCL/MD/034.

2.3.1.1. Nanoparticles and preparation. The NM-111 (BASF Z-Cote; Zincite ZnO NP functionalized with triethoxycaprylylsilane, 130 nm) was received from the European Commission Joint Research Centre repository (JRC, Ispra, Italy). Nanomaterials were sub-sampled and preserved under argon in the dark at room temperature until use. The details on raw material characteristics have been thoroughly examined previously within the same project (Kermanizadeh et al., 2013b). X-ray diffraction (XRD) size: 58–93 nm. BET surface area: 18 m^2/g. Via transmission electron microscopy (TEM) the size morphology was shown to be diverse; about 90% of particles with an aspect ratio of 1 were in the 20–200 nm size range and about 90% of particles with an aspect ratio between 2 and 8.5 were in the 10–450 nm size range.

With the following exceptions the preparation of the suspensions was identical as in study #1. The vehicle was composed of 0.5% EtOH (96%), 2% C57BL/6 mouse serum in MilliQ water. The stock suspension was prepared at 2 mg/mL and it was sonicated on ice (Virsonic 300 ultrasonic cell disrupter, Virtis, Gardiner, USA) for 16 min at an amplitude of 15%. The stock suspension was serially diluted in the same dispersion media and sonicated for 15 min in a water bath. Min-U-Sil was directly dispersed with the dispersion medium (no sonication).

2.3.1.2. Experimental design and exposure. Mice received a single pulmonary exposure dose of 12.5, 25, 50 and 100 μg ZnO NP/mouse or vehicle/negative control (N = 5). The positive control group consisted of 8 mice and was exposed to crystalline silica (2.5 mg Min-U-Sil/mouse; U.S. Silica Company, Berkeley Springs, USA), known to induce an inflammatory and fibrotic response. The vehicle control animals were exposed to 0.5% EtOH (96%), 2% C57BL/6 mouse serum in MilliQ water. The original experimental plan was for the sacrifice of mice 2 months post-exposure.

The particles were administered in the lungs by pharyngeal aspiration after 4% isoflurane for 30 s. NP suspensions at a fixed instillation volume of 50 μl, were deposited at the entrance of the trachea utilizing a pipette. At the first breath, the liquid was aerosolized and aspirated into the lungs of the mice.

2.3.1.3. Broncho-alveolar lavage fluid, cells and preparation of tissue. Mice were sacrificed 2 months after instillation with an overdose of sodium pentobarbital (15 mg/mouse intraperitoneally). Lungs were lavaged by the cannulation of the trachea and flushing lobes with 1 mL NaCl 0.9%. The lavage fluid was centrifuged (200 g, 10 min, 4 °C) and the cell-free supernatant was used for the measurement of LDH activity, protein content and quantification of selected cytokines. The measurement of LDH activity was performed using a Synchron LX Unicell DXC-800 (Beckman Coulter, Brea, USA) in the presence of 11 mM of NAD+ and 50 mM lactate. The total protein concentration was quantified spectrophotometrically at 600 nm after complexation with molybdate pyrogallol red. Finally, enzyme-linked immunosorbent assays (ELISA) were performed according to manufacturer's instructions (R&D Systems, Minneapolis, USA): TNFα, IL-1 α, IL-1 β, IL-6, IL-13, active transforming growth factor (TGF)-β1 and osteopontin (OPN) also called secreted phosphoprotein 1 (SPP-1).

The cell pellets were resuspended in NaCl 0.9%. BALF total cell number for each animal was determined in Turch (1% crystal violet (Merck, Darmstadt, Germany), 3% acetic acid). Cells were also pelleted onto glass slides by cytocentrifugation for differentiation by light microscopy after Diff-Quick staining (200 cells counted, Dade Behring AG, Düdingen, Switzerland).

Total pulmonary collagen was determined via OH-proline, an amino acid relatively specific for, and a major component of collagen. Following lavage, lungs were perfused with NaCl 0.9%, excised and placed in 3 mL ice-cold PBS. They were then homogenized on ice with an Ultra-Turrax T25 homogenizer (Janke & Kunkel, Brussels, Belgium) and stored at −80 °C. Part of the lung homogenate was hydrolyzed in HCl 6N at 108 °C during 24 h and OH-proline was quantified by high-performance liquid chromatography (Biondi et al., 1997).

Table 1
Body weight (g) of vehicle control mice and mice exposed to ZnO nanoparticles or Printex 90 at day of instillation (Day 0) and 2 and 3 days post-exposure.

	Instillation	Weight	Termination	Weight	Δ Weight	# Of mice
Control	Day 0	17.2 ± 0.3	Day 1	ND		12
ZnO 2 μg		17.8 ± 0.5		ND		6
ZnO 6 μg		18.3 ± 0.5		ND		6
ZnO 18 μg		17.8 ± 0.8		ND		6
P90 162 μg		17.6 ± 0.2		ND		6
Control	Day 0	18.5 ± 0.8	Day 2	19.2 ± 0.9	+0.7 g	2
ZnO 2 μg		17.2 ± 0.0		17.3 ± 0.0	+0.2 g	2
ZnO 6 μg		19.0 ± 0.5		17.0 ± 0.0	− 2.0 g*	2
ZnO 18 μg		18.2 ± 0.7		15.6 ± 0.7	− 2.6 g*	6
Control	Day 0	18.8 ± 0.5	Day 3	19.0 ± 0.5	+0.3 g	10
ZnO 2 μg		17.3 ± 0.7		17.5 ± 0.7	+0.2 g	4
ZnO 6 μg		18.3 ± 0.7		16.1 ± 0.7	− 2.2 g*	4
ZnO 18 μg		–		–	–	–
P90 162 μg		18.1 ± 0.4		18.4 ± 0.4	+0.3 g	6

Average weight of all 72 mice at the day of instillation 18 ± 1.3 g.
Results are given as mean ± SEM. P90; Printex 90 carbon black. ND: Not determined. Asterisks refer to statistical significance $^*p < 0.05$ when comparing to the relevant vehicle control.

Table 2
The cellular distribution in broncho-alveolar lavage fluid.

		Dose (μg)	Total #	Macrophages	Lymphocytes	Neutrophils	Eosinophils	Epithelial
		0	97,750 ± 12,177	75,430 ± 11,048	1104 ± 435	5349 ± 1155	715 ± 301	15,153 ± 2063
1 day		2	77,500 ± 6168	43,298 ± 3178	1118 ± 535	21,780 ± 2650	1663 ± 546	9643 ± 2176
	ZnO	6	80,500 ± 5277	34,078 ± 4437	848 ± 192	21,900 ± 4312	1238 ± 487	22,428 ± 3950
		18	94,000 ± 11,790	35,140 ± 7899	438 ± 206	35,083 ± 10516	188 ± 127	23,153 ± 3434
	P90	162	259,500 ± 27,086	27,803 ± 6113	1750 ± 1051	187,738 ± 16,959***	23,373 ± 9098	18,838 ± 6590
		0	87,600 ± 7332	72,090 ± 5931	1301 ± 441	582 ± 224	2621 ± 887	11,007 ± 1843
3 day		2	166,500 ± 42,294	121,556 ± 30,145	1436 ± 942	16,046 ± 2630	4991 ± 3563	17,126 ± 2818
	ZnO	6	454,500 ± 67,043***	12,7714 ± 28,954	15,105 ± 11,731**	271,170 ± 66,056***	7545 ± 3134	32,966 ± 12,220**
		18	–	–	–	–	–	–
	P90	162	222,500 ± 40,572***	69,338 ± 16,349	4180 ± 1562	76,930 ± 11,898**	56,983 ± 27,913***	15,070 ± 3278
Unexposed			67,125 ± 8017	57,602 ± 8194*	585 ± 192	746 ± 342	32 ± 32	8160 ± 713

All cells are listed in actual numbers. Results are given as mean ± SEM. P90; Printex 90 carbon black. ND: Not determined (terminated due to animal suffering). Asterisks refer to statistical significance **$p < 0.01$ and ***$p < 0.001$ when comparing to the relevant vehicle control. All samples were scored randomized.

Table 3
Red blood cells and concentration of protein in broncho-alveolar lavage fluid and DNA damage by the comet assay in the lavaged cells.

	Dose (μg)	RBC	Protein	Comet assay	# Animals
	0	0.5	312 ± 21	7.4 ± 0.9	12
1 day	2	0.8	522 ± 58	11.8 ± 1.6	6
ZnO	6	1.0	659 ± 76	13.4 ± 1.3*	6
	18	1.2	626 ± 91	14.9 ± 1.7***	6
P90	162	0.6	ND	8.2 ± 1.1	6
	0	0.6	301 ± 34	9.2 ± 0.7	10
3 day	2	0.3	574 ± 158	7.7 ± 0.8	4
ZnO	6	2.3***	4591 ± 1083***	6.8 ± 0.4	4
	18	–	–	–	–
P90	162	0.2	ND	12.6 ± 1.5	6
Unexposed		0.1	235 ± 20	8.1 ± 1.0	8

Results are given as mean or mean ± SEM. P90; Printex 90 carbon black. Not determined (terminated due to animal suffering). Asterisks refer to statistical significance *$p < 0.05$ and ***$p < 0.001$ when comparing to the relevant vehicle control. Red blood cells (RBC) were scored on a 4 tier scale (0–3): 0; non to very few RCB, 1; some RBC and 2; high levels of RBC and 3; very high levels of RBC. Proteins are presented as μg/ml. Comet as %Tail DNA. All samples were coded before analysis.

2.3.1.4. Statistical analysis for all 3 studies. All data are presented as mean values ± standard error of the mean (SEM). Differences were evaluated by using one-way analysis of variance followed by Sidak's test. Blood parameters (study 2) were analyzed by general linear model (GLM) followed by Sidak's test. Certain endpoints within study 2; macrophages, lymphocytes, neutrophils, CXCL-1, IL-6, CXCL-10 CXCL-5, G-CSF, MDA, Protein and LDH, and within study 3; total BAL cells, macrophages, lymphocytes and neutrophils displayed inhomogeneity of variance ($p < 0.05$, Bartlett's test). The statistical significance was confirmed using Kruskal–Wallis non-parametric test, whereas we have reported P-values of Sidak's tests for consistency in the manuscript. The mortality data was analyzed by χ^2. All statistical analysis was performed using STATA 13 (STATACORP LP, College station TX, USA) except for blood parameters which were analyzed using MiniTab 17 (Minitab Inc., State College, PA, USA).

3. Results

3.1. Study #1

The pilot study (2 mice, 162 μg ZnO NP) was terminated after about 30 h as the mice showed complete immobility and breathing difficulty. At autopsy it was shown that their lungs were filled with blood.

3.1.1. Body weight of mice

The weight of all mice was recorded immediately before the exposure and again at the termination day 2 and 3 (but not day 1).

Table 4
Type and incidence of histopathological changes in lungs and livers from mice 2 days post a single exposure of ZnO nanoparticles by intratracheal instillation.

Organ	Type of lesion	Control	Nano ZnO		
			2 μg	6 μg	18 μg
Lungs	Lymphoid cell infiltration of				
	alveolar lamina	0/2	1/2	1/2	0/2
	alveolar walls	0/2	0/2	2/2	0/2
	interstitium	0/2	1/2	1/2	1/2
	Excessive desquamation of bronchiole epithelium	0/2	2/2	1/2	2/2
	Hypertrophy of epithelial cells of bronchioles	0/2	2/2	0/2	2/2
	Proliferation of epithelial cells of bronchioles	0/2	0/2	1/2	0/2
	Oedema				
	alveolar walls	0/2	0/2	2/2	0/2
	subepithelial	0/2	0/2	1/2	0/2
	interstitial	0/2	0/2	0/2	1/1
	perivascular	0/2	0/2	0/2	2/2
	Congestion	2/2	2/2	2/2	2/2
Liver	Increased number of binucleate hepatocytes[a]	0/2	2/2	2/2	2/2
	Enlargement of single hepatocytes (hypertrophy)	0/2	1/2	1/2	2/2
	Necrosis of single hepatocytes	0/2	1/2	0/2	1/2
	Inflammatory cell focus	0/2	1/2	0/2	0/2
	Vacuolization of cytoplasm of hepatocytes (midzonal)	2/2	2/2	2/2	2/2
	Congestion	2/2	1/2	1/2	2/2

[a] Qualitative evaluation only.

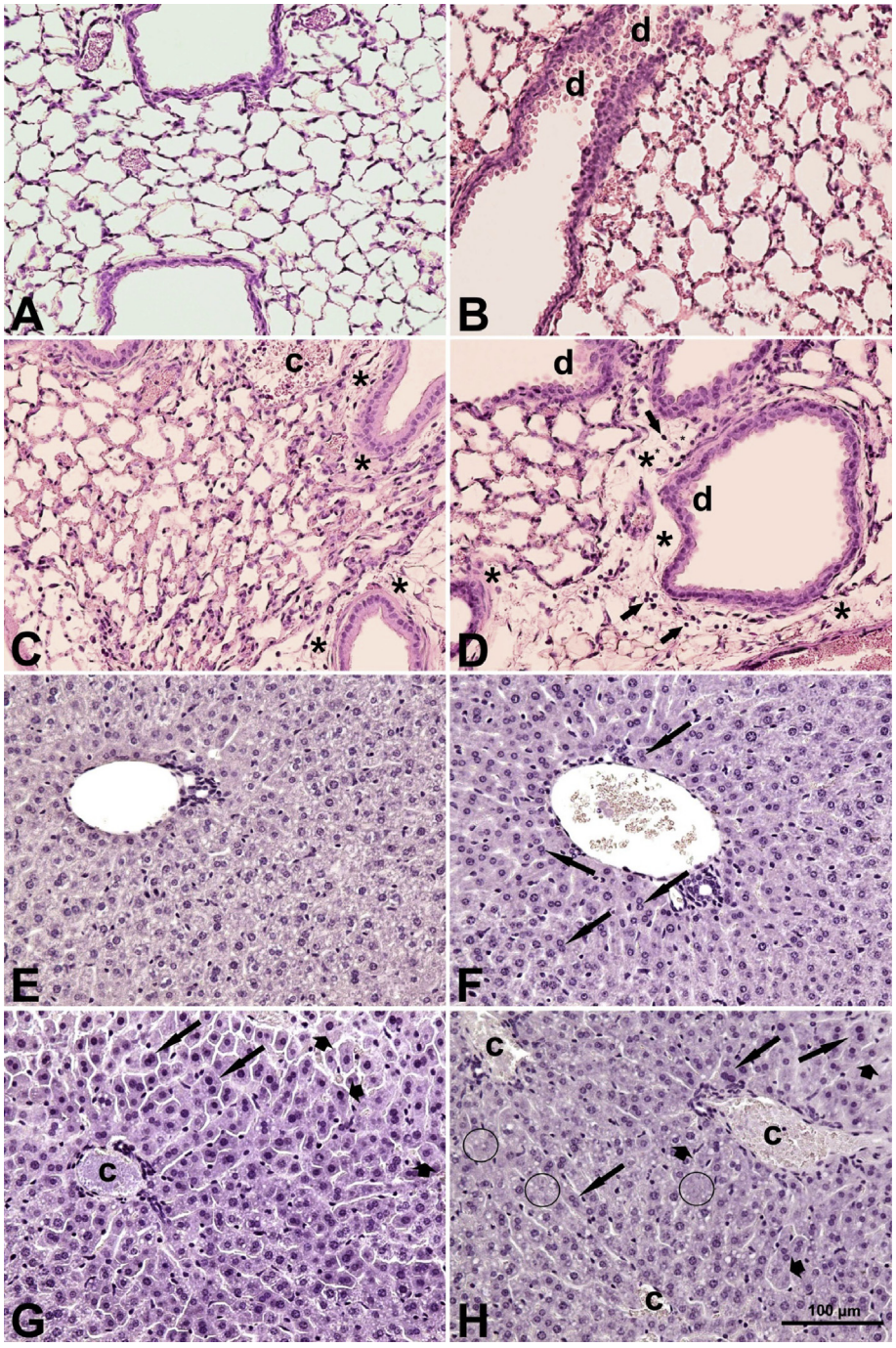

Fig. 1. Morphological patterns of the lung (A–D) and liver (E–H) in mice 2 days after intratracheal instillation of ZnO NP. A, E illustrate the normal structures in control animals. Slight vacuolization of hepatocyte cytoplasm (white spaces). B, F – mice exposed to 2 μg ZnO NP: desquamation (d) of the bronchiole epithelium, numerous binucleate hepatocytes (arrows); C, G – mice exposed to 6 μg ZnO NP: congestion (c), oedema (asterisks), numerous binucleate hepatocytes (arrows), slightly visible vacuolization of hepatocyte cytoplasm (white spaces), enlargement of hepatocytes (head of arrows); D, H – mice exposed to 18 μg ZnO NP: extensive interstitial oedema (asterisks), desquamation of the bronchiole epithelium (d), congestion (c), infiltration of lymphoid cells (short arrows), numerous binucleate hepatocytes (long arrows), enlargement of hepatocytes (head of arrows), intensive vacuolization of hepatocyte cytoplasm (white spaces), necrosis of the singles hepatocytes (in the circles). HE staining, magnifications were the same for all images as shown on image H.

The body weight significantly decreased by 14% at 2 days post-exposure in the group of mice that received 18 μg ZnO NP (Table 1). A decrease in body weight was also observed for mice exposed to 6 μg. Their weight significantly decreased by 11 and 12% at day 2 and 3 post-exposure, respectively. A marginal increase (between 0.9 and 3.8%) in body weight was observed for vehicle, 2 μg ZnO NP and Printex 90 exposed mice.

3.1.2. BALF: cellular composition, proteins and comet assay

The number and composition of cells in the lung lumen was assessed by NucleoCounter and microscopy (Table 2). One day post-exposure the results show a reduction in macrophages and an increase in neutrophils. However, three days post-exposure total cell numbers increased 2–5-fold for 2 and 6 μg exposures, respectively. This was mainly driven by a doubling of macrophages and a very

Table 5
Body weight and selected blood parameters.

1 Day	Dose (μg)	Body weight	WBC	Neutrophils	Lympho	Platelets	L-Platelets	Hematocrit	RBC
ZnO	0	−3.8 ± 0.7	7.3 ± 0.4	0.9 ± 0.1	6.1 ± 0.3	1072 ± 23	3.6 ± 0.8	49.7 ± 0.5	10.2 ± 0.1
	5	−5.2 ± 0.9	4.7 ± 0.5***	0.8 ± 0.1	3.7 ± 0.4***	979 ± 32	8.0 ± 1.1	50.2 ± 0.6	10.1 ± 0.1
	15	−11.0 ± 1.1***	4.3 ± 0.6***	1.9 ± 0.4***	2.3 ± 0.3***	1210 ± 58*	11.0 ± 2.9**	54.3 ± 2.2*	11.0 ± 0.4*
SiO_2	35	−3.8 ± 0.6	5.2 ± 0.3**	0.9 ± 0.1	4.1 ± 0.3***	1008 ± 39	6.3 ± 1.6	49.9 ± 0.6	10.2 ± 0.1
Unexposed		−4.4 ± 0.4	6.0 ± 0.4	0.8 ± 0.1	4.9 ± 0.3*	997 ± 24	2.4 ± 0.6	48.0 ± 0.5	9.8 ± 0.1

Body weights are listed as % reduction in body weight as compared to weight on the day of instillation. WBC (White blood cells), Neutrophils, Lympho (lymphocytes), Platelets, L-Platelets (large platelets) are listed in actual numbers ($\times 10^3$/μl blood). Hematocrit is in %. RBC (red blood cells $\times$ 10^6/μl blood). Results are given as mean ± SEM. SiO_2 is crystalline silica Min-U-Sil 5. Asterisks refer to statistical significance *p < 0.05, **p < 0.01 and ***p < 0.001 when comparing to the vehicle control (N = 8).

Table 6
The cellular distribution in broncho-alveolar lavage fluid.

1 Day	Dose (μg)	Total #	Macrophages	Lymphocytes	Neutrophils
ZnO	0	456,000 ± 33,000	423,000 ± 90,000	1800 ± 2200	31,300 ± 6800
	5	369,000 ± 32,000	321,000 ± 64,000	4200 ± 3100	43,900 ± 28,500
	15	523,000 ± 78000	233,000 ± 52,000*	10,100 ± 6000***	280,100 ± 175,200***
SiO_2	35	488,000 ± 49,000	293,000 ± 77,000	3000 ± 1400	192,100 ± 70,300**
Unexposed		486,000 ± 49,000	482,000 ± 143,000	0 ± 0	3700 ± 3500

All cells are listed in actual numbers. Results are given as mean ± SEM. SiO_2 is crystalline silica Min-U-Sil 5. Asterisks refer to statistical significance *p < 0.05, **p < 0.01 and ***p < 0.001 when comparing to the vehicle control (N = 8).

large increase in neutrophils (30 to 511-fold for 2 and 6 μg exposures, respectively). In addition to these large increases in macrophages and neutrophils, 6 μg exposed mice also showed an increase in lymphocytes (3-fold w/o, 12-fold with a high outlier) (Table 2). As these mice also displayed very high numbers of red blood cells in the BALF, these results indicate alveolar-capillary barrier damage with loss of membrane integrity (Table 3). This was further supported by the 15-fold increase in concentration of BALF proteins indicating cellular damage as well as serum protein leaking through the disrupted alveolar-capillary barrier into the pulmonary space. This is strongly exemplified by the steep increase in red blood cells present in the BALF and on the cytoslides from animals exposed to 6 μg ZnO NP 3 days post-exposure ($p < 0.001$).

Comet assay was used to determine possible DNA damage (strand breaks) in the BALF cells. The results indicate a dose dependent increase (1.6, 1.8 and 2-fold) for ZnO NP exposed mice one day post-exposure. However, three days post-exposure this was reduced to a marginal decrease in genotoxicity (Table 3).

3.1.3. Lung and liver histology by light microscopy

As mice exposed to 18 μg ZnO NP manifested severe clinical signs of toxicity (recumbency, immobility, pilo erection) 2 days post-exposure, it was decided to terminate this group (off schedule) and to perform a histopathological examination of lungs and liver from two mice in each of the groups 0, 2, and 6 μg ZnO NP/mouse. The rest of the mice were terminated as scheduled three days after exposure). Histological results are summarized in Table 4. As the animals were not exsanguinated, congestion was observed in all samples from lungs and livers.

An excessive desquamation of epithelial cells of bronchioles as compared to the controls was recorded in all but one ZnO NP exposed animals; the severity of the lesion varied between the treated animals without a clear dose response. Other changes indicative of pulmonary injury were oedema (perivascular, subepitelial, interstitial and/or of alveolar walls) in animals from mid and high ZnO NP dose groups, lymphoid cell infiltration of the interstitial tissue or in alveolar interstitium or lamina, and hypertrophy of single epithelial cells or proliferation of epithelial cells of bronchioles were recorded occasionally (Table 4).

In the livers from ZnO NP exposed animals the most noteworthy changes were an increased presence of binucleate hepatocytes and enlargement of single hepatocyte. Both these lesions are considered as indicative of a regenerative activity of liver tissue after exposure to a toxicant (Kostka et al., 2000). Mice exposed to 2 and 18 μg ZnO NP had necrosis of single hepatocytes. The number of recorded pathomorphological changes was similar in animals exposed to ZnO NP, however the changes appeared more severe in the animas exposed to 18 μg ZnO NP. Exemplified images of lung and livers from all exposure groups are shown in Fig. 1.

Table 7
Markers of tissue damage determined broncho-alveolar lavage fluid.

1 Day	Dose (μg)	LDH	Protein	IgM
ZnO	0	22.4 ± 7.5	138 ± 14	5.0 ± 1.3
	5	58.4 ± 13.0	148 ± 16	18.2 ± 9.2
	15	637.1 ± 95.2***	447 ± 30***	178.9 ± 6.9***
SiO_2	35	166.2 ± 36.1	138 ± 13	28.3 ± 8.7
Unexposed		28.6 ± 8.1	105 ± 5	14.0 ± 3.3

Results are given as mean ± SEM. SiO_2 is crystalline silica Min-U-Sil 5. LDH (Lactate dehydrogenase U/ml). Proteins (μg/ml). IgM (Immunoglobulin M pg/ml). Asterisks refer to statistical significance *p < 0.05, **p < 0.01 and ***p < 0.001 when comparing to the vehicle control (N = 8).

3.2. Study #2

3.2.1. Weight of mice

The experiment was stopped 24 h after exposure due to signs of distress and acute toxicity (reduced body weight, reduced mobility and pilo erection) in the 15 μg ZnO NP group. Body weight was determined on day of application and on day of dissection. Body weight loss was calculated as the difference between the day of dissection and the day of instillation. At 24 h the 15 μg ZnO NP group had an 11% reduced body weight ($p < 0.001$), whereas all other groups showed a marginal weight reduction of 4–5% (Table 5). This is a clear sign of acute poisoning in the high dose ZnO NP group.

3.2.2. Blood parameters

Systemic effects were determined via a hematological analysis of 45 parameters. The GLM ANOVA showed significant difference for 32 of the 45 blood parameters. The 32 parameters were tested post hoc and the high dose zinc group showed significant

Table 8
Cytokines assessed in broncho-alveolar lavage fluid.

1 Day	Dose (μg)	IL-6	CXCL-1	CXCL-10	CCL-2	G-CSF
ZnO	0	2.8 ± 0.0	27.3 ± 14.4	8.9 ± 4.7	5.6 ± 0.9	6.6 ± 1.1
	5	4.7 ± 3.3	25.3 ± 9.6	6.2 ± 0.0	10.5 ± 2.0	9.0 ± 7.1
	15	1356.1 ± 990.6**	349.9 ± 183.8***	108.3 ± 34.1***	37.3 ± 2.1***	1933.4 ± 374.2***
SiO_2	35	1.8 ± 1.0	175.9 ± 32.7	11.9 ± 8.8	11.1 ± 1.5	47.5 ± 8.3
Unexposed		2.8 ± 0.0	14.8 ± 2.5	5.5 ± 1.6	9.2 ± 1.5	3.5 ± 0.9
1 Day	Dose (μg)	TNFα	IL-1a	IL-10	CXCL-5	IFNγ
ZnO	0	0.8 ± 0.6	50.6 ± 10.0	38.7 ± 16.9	2.5 ± 0.0	9.2 ± 6.8
	5	1.2 ± 0.7	29.0 ± 10.3	10.6 ± 6.4	3.1 ± 1.0	3.8 ± 0.0
	15	2.4 ± 1.2	56.8 ± 9.4	46.2 ± 33.1	5.1 ± 4.5	12.0 ± 1.0
SiO_2	35	5.5 ± 1.5***	57.4 ± 11.7	26.7 ± 19.8	36.4 ± 11.1**	8.1 ± 6.7
Unexposed		1.1 ± 0.4	63.9 ± 5.6	35.1 ± 18.9	8.6 ± 7.7	9.8 ± 5.6

Results are given as mean ± SEM. SiO_2 is crystalline silica Min-U-Sil 5. All cytokines (pg/ml). Asterisks refer to statistical significance *p < 0.05, **p < 0.01 and ***p < 0.001 when comparing to the vehicle control (N = 8).

Table 9
Oxidative stress parameters determined in lung tissue.

1 Day	Dose (μg)	GSH	MDA	Catalase
ZnO	0	16.6 ± 0.7	16.7 ± 0.3	13.9 ± 0.5
	5	16.1 ± 0.6	17.5 ± 1.0	17.6 ± 0.4***
	15	12.4 ± 0.5***	30.4 ± 0.9***	13.2 ± 0.5
SiO_2	35	14.0 ± 0.4*	18.4 ± 0.8*	14.5 ± 0.2
Unexposed		15.8 ± 0.4	14.4 ± 0.4	14.4 ± 0.2

Results are given as mean ± SEM. SiO_2 is crystalline silica Min-U-Sil 5. GSH; glutathione (nmol/mg protein). MDA; malondialdehyde (nmol/100 mg protein). Catalase (U/mg protein). Asterisks refer to statistical significance *p < 0.05, **p < 0.01 and ***p < 0.001 when comparing to the vehicle control (N = 8).

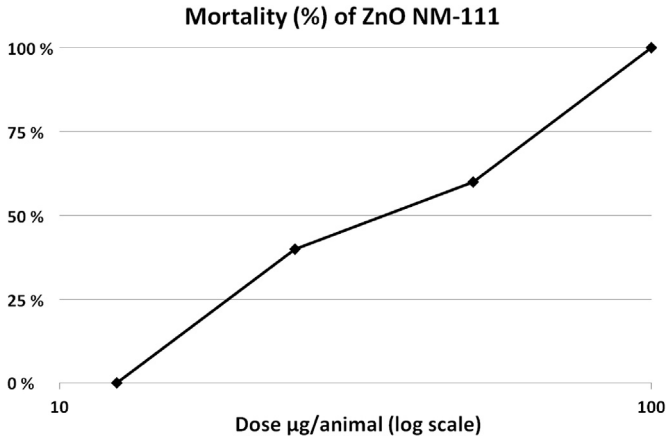

Fig. 2. Mortality curve for mice exposed to nanosized ZnO (N = 5).

difference in 28 of these parameters. The low dose zinc group showed significant difference in 11 parameters, whereas SiO_2 and unexposed controls showed significant difference in 6 and 1 parameter, respectively. Selected parameters are shown in Table 5.

A strong increase in neutrophils and a reduction in white blood cells and lymphocytes was observed for the 15 μg ZnO NP group as compared to vehicle control. Increased number of blood neutrophils is a clear sign for an acute systemic inflammatory response to the pulmonary injury caused by ZnO. The increase in neutrophils might be on the expense of lymphocytes which present the majority of white blood cells in mice (Table 5). This combined with a possible retention of activated leukocytes in the injured capillary bed of the lungs cause a temporal lymphopenia.

Acute inflammation is often accompanied by increased platelet production, resulting in increased platelet counts and enhanced blood coagulability. The presence of immature, large platelets and clumbs of activated platelets are the hematological signs observed during the acute phase of systemic inflammation. Platelet count ($p < 0.05$), large platelets ($p < 0.01$) and clumps count ($p < 0.05$; not shown) were all significant elevated in the 15 μg ZnO NP group indicating thrombocytosis/thrombocythemia (Table 5). No other group showed any statistically significant altered platelet status, although the low dose ZnO NP showed a marginal increase in large platelets.

Increased production of red blood cells (polycythemia) and raised hematocrit (Table 5) may be assumed as further systemic signs to pulmonary injury, as the body compensates insufficient oxygen absorption by producing more red blood cells.

3.2.3. BALF: cellular composition, LDH, protein, immunoglobulin M and cytokines

Cellular composition was determined by microscopy. A very strong pulmonary influx (9-fold) of neutrophils was observed in the 15 μg group 24 h post-exposure, accompanied by a reduction of macrophages to about half. There was no increase in neutrophils and only a marginal reduction in macrophages was observed for the 5 μg group (Table 6).

ZnO NP (15 μg) caused significant toxicity to lung. This was

Table 10
Cellular distribution in broncho-alveolar lavage fluid.

2 Months	Dose (μg)	Total #	Macrophages	Lymphocytes	Neutrophils	Eosinophils
ZnO	0	48,300 ± 14,181	34,235 ± 6089	7376 ± 3804	163 ± 94	6526 ± 4457
	12.5	49,400 ± 13,917	48,710 ± 13,828	499 ± 185	190 ± 101	0
	25	75,833 ± 16,220	72,857 ± 17,459	2975 ± 1291	0	0
	50	44,750 ± 9750	43,582 ± 9282	1031 ± 331	0	0
SiO_2	0	26,571 ± 2438	22,148 ± 2217	2450 ± 635	182 ± 71	1790 ± 671
	2500	80,062 ± 14,228*	54,237 ± 10,878	14,934 ± 3384*	9865 ± 1874***	1221 ± 497

All cells are listed in actual numbers. Results are given as mean ± SEM. SiO_2 is crystalline silica Min-U-Sil. Asterisks refer to statistical significance *p < 0.05 and ***p < 0.001 when comparing to the relevant vehicle control. Only animals that survived 2 months post-exposure was included. ZnP NP groups 0 and 12.5 μg (N = 5), ZnP NP group 25 μg (N = 3), ZnP NP group 50 μg (N = 2) and SiO_2 groups 0 and 2500 μg (N = 8).

Table 11
LDH, concentration of proteins, cytokines assessed in broncho-alveolar lavage fluid and hydroxyproline in lung tissue.

2 Months	Dose (μg)	LDH	Protein	IL-1β	IL-1α	IL-6
ZnO	0	54 ± 2.2	74 ± 8	5.0 ± 1.0	21.5 ± 5.5	16.6 ± 2.7
	12.5	56 ± 7.0	60 ± 5	3.7 ± 0.4	23.0 ± 3.1	13.7 ± 1.1
	25	47 ± 9.2	60 ± 6	3.5 ± 0.1	16.5 ± 1.1	11.8 ± 1.2
	50	41 ± 0.0	65 ± 5	3.5 ± 0.3	15.0 ± 0.2	11.6 ± 0.0
SiO_2	0	62 ± 10.2	54 ± 9	4.9 ± 2.3	22.6 ± 1.6	18.6 ± 1.6
	2500	130.4 ± 14.3**	155 ± 12***	4.5 ± 0.3	19.4 ± 1.2	19.6 ± 1.5
2 months	Dose (μg)	TNFα	IL-13	TGF-β1	OPN	OH-Proline
ZnO	0	29.7 ± 7.7	6.0 ± 3.4	47.3 ± 11.6	20,999 ± 5392	254 ± 14
	12.5	43.1 ± 11.6	2.5 ± 0.6	40.8 ± 4.5	11,508 ± 917	259 ± 20
	25	13.5 ± 1.1	1.5 ± 0.0	32.9 ± 4.1	10,963 ± 699	276 ± 7
	50	24.8 ± 3.4	1.6 ± 0.0	55.9 ± 10	16,624 ± 1644	363 ± 54*
SiO_2	0	59.3 ± 13.4	5.2 ± 1.2	52.3 ± 6.0	16,372 ± 2197	191 ± 23
	2500	26.2 ± 5.8	4.6 ± 0.3	80.4 ± 14.4	76,201 ± 8450	281 ± 12**

Results are given as mean ± SEM. SiO_2 is crystalline silica Min-U-Sil. LDH (U/l); Protein (μg/ml); Cytokines (pg/ml). Asterisks refer to statistical significance *$p < 0.05$, **$p < 0.01$ and ***$p < 0.001$ when comparing to the relevant vehicle control. Only animals that survived 2 months post-exposure was included. ZnP NP groups 0 and 12.5 μg (N = 5), ZnP NP group 25 μg (N = 3), ZnP NP group 50 μg (N = 2) and SiO_2 groups 0 and 2500 μg (N = 8).

illustrated by a strong increase in LDH (28-fold, $p < 0.001$) caused by cell and tissue damage. Additionally, increased epithelial-endothelial permeability and cell leakage was shown by elevated concentration of BALF proteins (3-fold; $p < 0.001$). There was a 36-fold ($p < 0.001$) increase in Immunoglobulin M (IgM) in BALF 24 h post-exposure in the high dose group. IgM is the largest antibody in the bloodstream and the first antibody to appear in response to initial antigen exposure. IgM accumulation in BALF may indicate an injury to the alveolar barrier allowing the leakage of large serum proteins into the alveolar space (IgM is 970 kDa). Only minor differences were observed for the low dose group (5 μg) (Table 7).

Overall, treatment with 15 μg of ZnO NP caused a dramatic increase in expression of pro-inflammatory cytokine IL-6 (484-fold) as well as chemotactic cytokines such as CXCL-1 (KC) and CCL-2 (MCP-1) involved in the recruitment of neutrophils and monocytes/macrophages, respectively, to the site of inflammation. The latter two increased by 13- and 7-fold, respectively. Additionally, G-CSF and CXCL-10 which also may be involved in maintaining pulmonary inflammation, enhancing granulocyte survival and attraction of monocytes/macrophages and T cells were significantly elevated 293- and 12-fold, respectively. Elevated levels of CCL-2 and CXCL-10 have been associated with pulmonary fibrosis, although CCL-2 is a known fibrocyte chemoattractant (Murray et al., 2008), exogenous CXCL-10 inhibited fibrogenesis (Jiang et al., 2010). CCL-2 may promote fibrogenesis whereas CXCL-10 may act antifibrogenic. Finally, no significant changes in expression of TNFα, IL-1α and the anti-inflammatory cytokine IL-10, CXCL-5 and IFNγ were observed for any of the groups (Table 8).

3.2.4. Oxidative stress in lung tissue

Oxidative stress markers assessed in lung tissue, reflected depletion of the antioxidant glutathione (GSH), levels of the lipid peroxidation product malondialdehyde (MDA), and activity of the antioxidant enzyme catalase. For the high dose ZnO NP (15 μg) a significant decrease in GSH accompanied by a significant increase in MDA levels was observed, while, catalase activity was unaltered. The 5 μg group showed the opposite with no change in GSH and MDA but with a significant increase in catalase activity (Table 9).

3.3. Study #3

3.3.1. Mortality

Mice were exposed once to NM-111 ZnO NP by oro-pharyngeal aspiration. Animal mortality was observed for some doses. All 5 mice in the 100 μg/mouse group and 3 mice in the 50 μg/mouse group died within 5 days post-exposure. Two mice in the 25 μg/mouse group died within 13 days post-exposure. None of the mice in the 12.5 μg/mouse, negative control or positive control (crystalline silica) groups died prior to scheduled termination (Fig. 2). There was a strong association between ZnO NP dose and mortality ($p < 0.01$; $\chi^2 = 15$).

3.3.2. BALF: cellular composition, LDH, proteins and cytokines

Only animals that survived 2 months post-exposure were included in these analyses. This weakens the statistical power. The number and composition of cells in the BALF was not significantly changed for any of the ZnO NP exposure groups 2 months post-exposure (Table 10). There was a small increase of macrophages, but almost no neutrophils, lymphocytes or eosinophils were present. The 25 μg group showed marginally higher levels of some cell types. However, the % distribution of these cell types was almost identical to the other ZnO NP groups.

The integrity of pulmonary cells and the alveolar-capillary membrane barrier was evaluated via LDH activity and total protein levels in the BALF. However, ZnO NP had no effect on these parameters two months post-exposure in the surviving animals (Table 11).

Cytokines and growth factors were assessed in BALF by ELISA. ZnO NP had no significant effect on the pro-inflammatory cytokines IL-1α, IL-1β, TNFα and IL-6, the pro-fibrotic TGF- β1 or the cytokines IL-13 and OPN, in surviving animals. All protein levels were similar or marginally lowered compared to vehicle control exposed mice (Table 11).

3.3.3. Pulmonary fibrosis

A potential fibrotic response was assessed via the hydroxyproline lung content, a marker for collagen accumulation. ZnO NP induced a marginal (low doses) and significant (50 μg) induction of collagen. However, although significant for high dose group, it should be noted that 3 mice died shortly after intratracheal instillation in this group. Thus only 2 mice are represented in the 50 μg group 2 months post-exposure. The fold increase in hydroxyproline was similar for 50 μg ZnO NP and 2500 μg SiO_2 (1.4 and 1.5-fold, respectively) (Table 11).

4. Discussion

NP are mobile, easily inhaled and can deposit in the pulmonary alveoli at a much higher frequency than larger bulk sized particles. Although literature on hazards related to inhalation of nanosized

ZnO is available, information on lung toxicity is still limited and the doses used are primarily low. Here we present results from three experiments that each investigate the acute or sub-acute pulmonary toxicity of nanosized ZnO. The pulmonary toxicity is characterized by oxidative stress, inflammation, genotoxicity and cell death. Doses used in the present publication spanned from 2 to 100 μg/mouse (162 μg in the pilot study).

The most pronounced effect observed following the ZnO NP exposure was the clear association between exposure dose and mortality (Study 3). A mortality rate of 40% was observed at a bolus dose of 25 μg (~1.4 mg/kg mouse body weight) and increasing to 100% at a dose of 100 μg. Mortality caused by pulmonary exposure to ZnO particles has to the best of our knowledge not been reported previously in the literature. The currently available reports on ZnO toxicity in animal models have used sub-lethal doses, too short post-exposure time, or moribund/dead animals have not been included in the biochemical and histopathological examinations. However, LD_{50} for ZnO NP was calculated to be 0.3 mg/kg in intravenously exposed ICR mice (Fujihara et al., 2015). Also mortality has been reported following high peritoneal exposure (80 mg/kg body weight) of ZnO ≤ 200 nm in rats (Landsiedel et al., 2010) and a high oral NP exposure in mice (333 mg/kg body weight) (Esmaeillou et al., 2013). The highest pulmonary exposure dose found in the literature is 50 mg instilled in guinea pigs (222 mg/kg guinea pig body weight). Although, these particles were very large (<5000 nm) leading to a slow dissolution of Zn(II), species specific differences in the toxic response cannot be excluded (Gupta et al., 1986). Also no mortality or reduced body weight was observed when ZnO NP was instilled at a dose of 10 mg/rat (37 mg/kg body weight) (Chuang et al., 2014) or when ZnO NP was given as multiple instillations of 17.5 mg/kg rat every second day for five weeks (Liu et al., 2013). In our study mice exposed to 6 and 18 μg (study 1) and 15 μg (study 2) showed a significant decrease in body weight of more than 10%. It should be noted that a clear difference in toxicity towards ZnO fumes has been observed in a test of 11 different inbred mouse strains (Wesselkamper et al., 2001) making interspecies difference very likely. It is especially noteworthy that C57BL/6J (C57BL/6J and C57BL/6N was used in study 1 and 3, respectively) was amongst the lowest responders with regards to inflammation (PMNs) (10-fold) and protein concentration (1.1-fold) in BALF following a single inhalation exposure vs air exposed controls. BALB/c mice (similar to study 2) were more sensitive than C57BL/6 in terms of these parameters. These results indicate that even stronger responses might have been observed in our studies if high responder strains had been used, e.g. C3H/HeOuJ and CBA/J mice which showed a 555 and 420-fold increase in PMNs and a 3 and 2.4-fold increase in protein concentration vs air exposed controls (Wesselkamper et al., 2001).

We hypothesize that leakage of fluids to the lung is the direct or at least partial cause for the observed mortality. In the pilot study, within study 1, two mice were exposed to 162 μg ZnO NP. These mice were killed off schedule after about 30 h. Their lungs were completely filled with blood. Although at much lower levels, mice exposed to 6 μg (study 1) showed epithelial damage, desquamation and a concomitantly increased barrier permeability of the alveolar/blood (2–3 days post-exposure). This was especially evident by the large increase in red blood cells and protein in BALF. Results from study 2 support these findings. Mice exposed to 15 μg showed a strong increase in LDH, protein and IgM in BALF 1d post-exposure. Similar results are generally observed in the literature (Ho et al., 2011; Chuang et al., 2014) and are indicative of strong pulmonary toxicity with cell death and injury to the alveolar barrier allowing fluids to enter the pulmonary space. Indeed, the detailed and dramatic cell death of alveolar epithelial cells, and therefore barrier destruction has been studied *in vitro* (LA4-alverolar epithelial cells). Toxicity was observed starting at very low concentrations (≥3 μg/ml ZnO NP) and was not observed with e.g. ≤500 μg crystalline silica (Min-U-Sil 5) (Beyerle et al., 2010). However, as mentioned above mice have died from ZnO exposure via other routes; e.g. an LD_{50} of 0.3 mg ZnO NP/kg body weight indicates other toxic mechanisms not related to leakage of fluid into the pulmonary space.

Available data show that it is dissolution of Zn(II) ions from the particles that is the major determinant for ZnO-mediated toxicity and cell death (Landsiedel et al., 2014). Accordingly, NP are more toxic than larger counterparts as the dissolution rate increases with decreasing particle size (Meulenkamp, 1998). Additionally, ZnO purity is important as e.g. dissolution is reduced by doping ZnO NP with iron (Xia et al., 2011). Uptake in acidic endosomes and later lysosomes accelerate dissolution leading to lysosomal damage, mitochondrial disturbance, production of ROS and cytokines (Nel et al., 2009). Similar effects have been observed in human cell lines (Kao et al., 2012). In Cho and co-workers detailed work the authors hypothesized that a rapid dissolution of ZnO NP inside endosomes/lysosomes is the primary cause for severe lung injury caused by ZnO NP (Cho et al., 2011). It is worth mentioning that the mortality was observed in study 3 using the largest particle of the 3 studies (130 nm vs 12 and 70 nm in study 1 and 2, respectively). Mortality was not observed in study 1 and 2 as these studies were short term. However, this indicates that even stronger responses (higher mortality) might have been observed in study 3 if even smaller NP were used.

Mice surviving the initial exposure of ZnO NP up to 25 μg (~1.35 mg/kg mouse body weight) appeared to have no effects assessed on a number of markers of pulmonary inflammation and barrier integrity 2 months post-exposure. However a dose of 50 μg (~2.7 mg/kg mouse body weight) caused increased collagen accumulation in the lungs. Fibrosis was identified at a time point when all inflammatory end-points were similar to control levels indicating a resolved inflammation. Additionally, the levels of collagen were similar after exposure to 50 μg ZnO NP and 2500 μg crystalline silica. Cho and co-workers have previously shown that aspiration of 310 μg ZnO NP (~1.4 mg/kg rat body weight) caused "severe fibrosis and airway epithelial injury" and that the mechanism likely involved Zn(II) ions. Instillation of Zn(II) ions (92.5 μg) caused both fibrosis and mortality (Cho et al., 2011).

In general ZnO NP caused a very strong inflammatory response with neutrophils increasing between 4-and 7-fold in study 1 (2, 6 and 18 μg) and between 1.4 and 9-fold in study 2 (5 and 15 μg) 1d post-exposure. End-points determined in study 1 and 2 (18 μg and 15 μg, 24 h post-exposure) were similar in fold-inductions with a marginal tendency to stronger results in study 2 neutrophils, lymphocytes and protein. Since study 1 incorporated a smaller particle (12 nm vs 70 nm) and slightly larger dose (18 μg vs 15 μg) the differences might be caused by the more responsive BALB/c mice used in study 2. Inflammation is not in itself problematic if it is resolved quickly. However, if not resolved inflammation may lead to oxidative stress; an imbalance between production of reactive oxygen/nitrogen species and antioxidant defense systems. Both inflammation and oxidative stress are important mechanisms implicated in particle-induced health effects such as cancer and systemic effects (Moller et al., 2010, 2014, 2015). Whilst oxidative stress markers are frequently assessed *in vitro* with ZnO they are very seldom assessed in animal studies. Markers of oxidative stress were determined in our study 2, where 15 μg of ZnO NP caused a significant increase of lipid oxidation and decrease of the antioxidant glutathione. The antioxidant enzyme catalase was increased at the low dose but not in the high dose group. It is possible that low doses of ZnO induce the antioxidant response via the Nrf2 pathway and thus the expression of catalase, whereas larger doses of ZnO NP

may deplete it. We also found that the local milieu affects genome integrity. DNA damage was observed in the BALF cells 1d post-exposure. However, this effect was not present 3d post-exposure. Previously short term *in vitro* exposures have shown that ZnO NP is a potent inducer of strand breaks and oxidatively damaged DNA determined by comet assay (Gerloff et al., 2009).

Pulmonary exposure to ZnO also caused systemic effects. Several blood parameters indicative of acute systemic inflammation was altered in the 15 μg ZnO NP group. Histology of the liver showed an increased regenerative activity by the presence of binucleated hepatocytes and enlargement of single hepatocyte. In both study 1 and 2 systemic effects were stronger in animals receiving the high dose (18 and 15 μg, respectively).

In summary, a bolus pulmonary exposure of 6 μg ZnO NP (0.3 mg/kg mouse body weight) manifested severe signs of toxicity in terms of reduced body weight, large acute pulmonary inflammation and excessive desquamation of epithelial cells with concomitant leakage of the alveolar barrier. Additionally, histology revealed increased proliferation and hypertrophy of bronchiole epithelial cells as well as lymphoid cell infiltration and oedema. Increased number of binucleated cells and hypertrophy was evident in the liver indicating systemic effects of a pulmonary bolus dose of 6 μg ZnO NP. Higher doses of 15 and 18 μg ZnO NP yielded stronger effects and animal suffering which lead to the termination of experiments (study 1 and 2). Even higher bolus doses of ZnO NP were clearly associated with a dose dependent mortality (≥25 up to 100 μg) and with collagen accumulation indicative of pulmonary fibrosis (50 μg).

Conflicts of interest

The authors report no competing interests.

Acknowledgment

The authors indebted and thanks Michael Guldbrandsen, Anne-Karin Asp, Elzbieta Christiansen, Lourdes M. Pedersen (National Research Centre for the Working Environment), Kathrin Kappes (Helmholtz Zentrum München), Sarah Grundt Simonsen (National Food Institute, Technical University of Denmark) and Aleksander Penkowski (University of Warmia and Mazury in Olsztyn) for their excellent technical assistance. The project was supported by Danish Centre for Nanosafety, grant# 20110092173-3 from the Danish Working Environment Research Foundation, the E.C. FP7 ENPRA (n°228789) grant, the E.C. FP7 Nanosustain (n°247989) and the E.C. FP7 NanoValid (n°263147).

Transparency document

Transparency document related to this article can be found online at http://dx.doi.org/10.1016/j.fct.2015.08.008.

References

Banerjee, A., Trueblood, M.B., Zhang, X., Manda, K.R., Lobo, P., Whitefield, P.D., Hagen, D.E., Ercal, N., 2009. N-acetylcysteineamide (NACA) prevents inflammation and oxidative stress in animals exposed to diesel engine exhaust. Toxicol. Lett. 187, 187–193.

Baxter, J.B., Aydil, E.S., 2005. Nanowire-based dye sensitized solar cells. Appl. Phys. Lett. 86, 053114.

Beyerle, A., Irmler, M., Beckers, J., Kissel, T., Stoeger, T., 2010. Toxicity pathway focused gene expression profiling of PEI-based polymers for pulmonary applications. Mol. Pharm. 7, 727–737.

Beyerle, A., Braun, A., Merkel, O., Koch, F., Kissel, T., Stoeger, T., 2011. Comparative in vivo study of poly(ethylene imine)/siRNA complexes for pulmonary delivery in mice. J. Control Release 151, 51–56.

Beyerle, A., Braun, A., Banerjee, A., Ercal, N., Eickelberg, O., Kissel, T.H., Stoeger, T., 2011. Inflammatory responses to pulmonary application of PEI-based siRNA nanocarriers in mice. Biomaterials 32, 8694–8701.

Biondi, P.A., Chiesa, L.M., Storelli, M.R., Renon, P., 1997. A new procedure for the specific high-performance liquid chromatographic determination of hydroxyproline. J. Chromatogr. Sci. 35, 509–512.

Bourdon, J.A., Saber, A.T., Jacobsen, N.R., Jensen, K.A., Madsen, A.M., Lamson, J.S., Wallin, H., Moller, P., Loft, S., Yauk, C.L., Vogel, U.B., 2012. Carbon black nanoparticle instillation induces sustained inflammation and genotoxicity in mouse lung and liver. Part. Fibre Toxicol. 9, 5.

Cho, W.S., Duffin, R., Howie, S.E., Scotton, C.J., Wallace, W.A., MacNee, W., Bradley, M., Megson, I.L., Donaldson, K., 2011. Progressive severe lung injury by zinc oxide nanoparticles; the role of Zn2+ dissolution inside lysosomes. Part. Fibre Toxicol. 8, 27.

Chuang, H.C., Juan, H.T., Chang, C.N., Yan, Y.H., Yuan, T.H., Wang, J.S., Chen, H.C., Hwang, Y.H., Lee, C.H., Cheng, T.J., 2014. Cardiopulmonary toxicity of pulmonary exposure to occupationally relevant zinc oxide nanoparticles. Nanotoxicology 8, 593–604.

Danielsen, P.H., Cao, Y., Roursgaard, M., Moller, P., Loft, S., 2014. Endothelial cell activation, oxidative stress and inflammation induced by a panel of metal-based nanomaterials. Nanotoxicology 1–12. http://dx.doi.org/10.3109/17435390.2014.980449.

Das, A., Wang, D.Y., Leuteritz, A., Subramaniam, K., Greenwell, H.C., Wagenknecht, U., Heinrich, G., 2011. Preparation of zinc oxide free, transparent rubber nanocomposites using a layered double hydroxide filler. J. Mater. Chem. 21, 7194–7200.

Esmaeillou, M., Moharamnejad, M., Hsankhani, R., Tehrani, A.A., Maadi, H., 2013. Toxicity of ZnO nanoparticles in healthy adult mice. Environ. Toxicol. Pharmacol. 35, 67–71.

Fujihara, J., Tongu, M., Hashimoto, H., Yamada, T., Kimura-Kataoka, K., Yasuda, T., Fujita, Y., Takeshita, H., 2015. Distribution and toxicity evaluation of ZnO dispersion nanoparticles in single intravenously exposed mice. J. Med. Invest. 62, 45–50.

Gerloff, K., Albrecht, C., Boots, A.W., Förster, I., Schins, R.P., 2009. Cytotoxicity and oxidative DNA damage by nanoparticles in human intestinal Caco-2 calls. Nanotoxicology 3, 355–364.

Gupta, S., Pandey, S.D., Misra, V., Viswanathan, P.N., 1986. Effect of intratracheal injection of zinc oxide dust in guinea pigs. Toxicology 38, 197–202.

Ho, M., Wu, K.Y., Chein, H.M., Chen, L.C., Cheng, T.J., 2011. Pulmonary toxicity of inhaled nanoscale and fine zinc oxide particles: mass and surface area as an exposure metric. Inhal. Toxicol. 23, 947–956.

Hogsberg, T., Jacobsen, N.R., Clausen, P.A., Serup, J., 2013. Black tattoo inks induce reactive oxygen species production correlating with aggregation of pigment nanoparticles and product brand but not with the polycyclic aromatic hydrocarbon content. Exp. Dermatol. 22, 464–469.

Jackson, P., Hougaard, K.S., Boisen, A.M., Jacobsen, N.R., Jensen, K.A., Moller, P., Brunborg, G., Gutzkow, K.B., Andersen, O., Loft, S., Vogel, U., Wallin, H., 2012. Pulmonary exposure to carbon black by inhalation or instillation in pregnant mice: effects on liver DNA strand breaks in dams and offspring. Nanotoxicology 6, 486–500.

Jacobsen, N.R., Saber, A.T., White, P., Moller, P., Pojana, G., Vogel, U., Loft, S., Gingerich, J., Soper, L., Douglas, G.R., Wallin, H., 2007. Increased mutant frequency by carbon black, but not quartz, in the lacZ and cII transgenes of muta(trade mark)mouse lung epithelial cells. Environ. Mol. Mutagen. 48, 451–461.

Jacobsen, N.R., Pojana, G., White, P., Møller, P., Cohn, C.A., Korsholm, K.S., Vogel, U., Marcomini, A., Loft, S., Wallin, H., 2008. Genotoxicity, cytotoxicity, and reactive oxygen species induced by single-walled carbon nanotubes and C60 in the FE1-Muta(TM) Mouse lung epithelial cells. Environ. Mol. Mutagen. 49, 476–487.

Jacobsen, N.R., Moller, P., Jensen, K.A., Vogel, U., Ladefoged, O., Loft, S., Wallin, H., 2009. Lung inflammation and genotoxicity following pulmonary exposure to nanoparticles in ApoE-/- mice. Part Fibre.Toxicol. 6, 2.

Jacobsen, N.R., White, P.A., Gingerich, J., Moller, P., Saber, A.T., Douglas, G.R., Vogel, U., Wallin, H., 2011. Mutation spectrum in FE1-MUTA(TM) Mouse lung epithelial cells exposed to nanoparticulate carbon black. Environ. Mol. Mutagen. 52, 331–337.

Jiang, D., Liang, J., Campanella, G.S., Guo, R., Yu, S., Xie, T., Liu, N., Jung, Y., Homer, R., Meltzer, E.B., Li, Y., Tager, A.M., Goetinck, P.F., Luster, A.D., Noble, P.W., 2010. Inhibition of pulmonary fibrosis in mice by CXCL10 requires glycosaminoglycan binding and syndecan-4. J. Clin. Invest. 120, 2049–2057.

Kao, Y.Y., Chen, Y.C., Cheng, T.J., Chiung, Y.M., Liu, P.S., 2012. Zinc oxide nanoparticles interfere with zinc ion homeostasis to cause cytotoxicity. Toxicol. Sci. 125, 462–472.

Karlsson, H.L., Gliga, A.R., Calleja, F.M., Goncalves, C.S., Wallinder, I.O., Vrieling, H., Fadeel, B., Hendriks, G., 2014. Mechanism-based genotoxicity screening of metal oxide nanoparticles using the Tox Tracker panel of reporter cell lines. Part. Fibre Toxicol. 11, 41.

Kermanizadeh, A., Gaiser, B.K., Hutchison, G.R., Stone, V., 2012. An in vitro liver model–assessing oxidative stress and genotoxicity following exposure of hepatocytes to a panel of engineered nanomaterials. Part Fibre.Toxicol. 9, 28.

Kermanizadeh, A., Vranic, S., Boland, S., Moreau, K., Baeza-Squiban, A., Gaiser, B.K., Andrzejczuk, L.A., Stone, V., 2013. An in vitro assessment of panel of engineered nanomaterials using a human renal cell line: cytotoxicity, pro-inflammatory response, oxidative stress and genotoxicity. BMC Nephrol. 14, 96.

Kermanizadeh, A., Pojana, G., Gaiser, B.K., Birkedal, R., Bilanicova, D., Wallin, H., Jensen, K.A., Sellergren, B., Hutchison, G.R., Marcomini, A., Stone, V., 2013. In vitro assessment of engineered nanomaterials using a hepatocyte cell line:

cytotoxicity, pro-inflammatory cytokines and functional markers. Nanotoxicology 7, 301–313.
Kostka, G., Palut, D., Kopec-Szlezak, J., Ludwicki, J.K., 2000. Early hepatic changes in rats induced by permethrin in comparison with DDT. Toxicology 142, 135–143.
Kumar, A., Dhawan, A., 2013. Genotoxic and carcinogenic potential of engineered nanoparticles: an update. Arch. Toxicol. 87, 1883–1900.
Kyjovska, Z.O., Jacobsen, N.R., Saber, A.T., Bengtson, S., Jackson, P., Wallin, H., Vogel, U., 2015a. DNA damage following pulmonary exposure by instillation to low doses of carbon black (Printex 90) nanoparticles in mice. Environ. Mol. Mutagen. 56, 41–49.
Kyjovska, Z.O., Jacobsen, N.R., Saber, A.T., Bengtson, S., Jackson, P., Wallin, H., Vogel, U., 2015b. DNA strand breaks, acute phase response and inflammation following pulmonary exposure by instillation to the diesel exhaust particle NIST1650b in mice. Mutagenesis. http://dx.doi.org/10.1093/mutage/gev009.
Landsiedel, R., Ma-Hock, L., Van, R.B., Schulz, M., Wiench, K., Champ, S., Schulte, S., Wohlleben, W., Oesch, F., 2010. Gene toxicity studies on titanium dioxide and zinc oxide nanomaterials used for UV-protection in cosmetic formulations. Nanotoxicology 4, 364–381.
Landsiedel, R., Sauer, U.G., Ma-Hock, L., Schnekenburger, J., Wiemann, M., 2014. Pulmonary toxicity of nanomaterials: a critical comparison of published in vitro assays and in vivo inhalation or instillation studies. Nanomedicine. (Lond.) 9, 2557–2585.
Lenz, A.G., Karg, E., Brendel, E., Hinze-Heyn, H., Maier, K.L., Eickelberg, O., Stoeger, T., Schmid, O., 2013. Inflammatory and oxidative stress responses of an alveolar epithelial cell line to airborne zinc oxide nanoparticles at the air-liquid interface: a comparison with conventional, submerged cell-culture conditions. Biomed. Res. Int. 2013, 652632.
Liu, H., Yang, D., Yang, H., Zhang, H., Zhang, W., Fang, Y., Lin, Z., Tian, L., Lin, B., Yan, J., Xi, Z., 2013. Comparative study of respiratory tract immune toxicity induced by three sterilisation nanoparticles: silver, zinc oxide and titanium dioxide. J. Hazard. Mater. 248–249, 478–486.
Ma, H., Williams, P.L., Diamond, S.A., 2013. Ecotoxicity of manufactured ZnO nanoparticles–a review. Environ. Pollut. 172, 76–85.
Meulenkamp, E.A., 1998. Size dependence of the dissolution of ZnO nanoparticles. J. Phys. Chem. B 102, 7764–7769.
Moller, P., Jacobsen, N.R., Folkmann, J.K., Danielsen, P.H., Mikkelsen, L., Hemmingsen, J.G., Vesterdal, L.K., Forchhammer, L., Wallin, H., Loft, S., 2010. Role of oxidative damage in toxicity of particulates. Free Radic. Res. 44, 1–46.
Moller, P., Christophersen, D.V., Jensen, D.M., Kermanizadeh, A., Roursgaard, M., Jacobsen, N.R., Hemmingsen, J.G., Danielsen, P.H., Cao, Y., Jantzen, K., Klingberg, H., Hersoug, L.G., Loft, S., 2014. Role of oxidative stress in carbon nanotube-generated health effects. Arch. Toxicol. 88, 1939–1964.
Moller, P., Jensen, D.M., Christophersen, D.V., Kermanizadeh, A., Jacobsen, N.R., Hemmingsen, J.G., Danielsen, P.H., Karottki, D.G., Roursgaard, M., Cao, Y., Jantzen, K., Klingberg, H., Hersoug, L.G., Loft, S., 2015. Measurement of oxidative damage to DNA in nanomaterial exposed cells and animals. Environ. Mol. Mutagen. 56, 97–110.
Murray, L.A., Argentieri, R.L., Farrell, F.X., Bracht, M., Sheng, H., Whitaker, B., Beck, H., Tsui, P., Cochlin, K., Evanoff, H.L., Hogaboam, C.M., Das, A.M., 2008. Hyper-responsiveness of IPF/UIP fibroblasts: interplay between TGFbeta1, IL-13 and CCL2. Int. J. Biochem. Cell Biol. 40, 2174–2182.
Nel, A.E., Madler, L., Velegol, D., Xia, T., Hoek, E.M., Somasundaran, P., Klaessig, F., Castranova, V., Thompson, M., 2009. Understanding biophysicochemical interactions at the nano-bio interface. Nat. Mater. 8, 543–557.
Nicklas, W., Baneux, P., Boot, R., Decelle, T., Deeny, A.A., Fumanelli, M., Illgen-Wilcke, B., 2002. Recommendations for the health monitoring of rodent and rabbit colonies in breeding and experimental units. Lab. Anim. 36, 20–42.
Pan, Z.W., Dai, Z.R., Wang, Z.L., 2001. Nanobelts of semiconducting oxides. Science 291, 1947–1949.
Pinnell, S.R., Fairhurst, D., Gillies, R., Mitchnick, M.A., Kollias, N., 2000. Microfine zinc oxide is a superior sunscreen ingredient to microfine titanium dioxide. Dermatol. Surg. 26, 309–314.
Poulsen, S.S., Saber, A.T., Williams, A., Andersen, O., Kobler, C., Atluri, R., Pozzebon, M.E., Mucelli, S.P., Simion, M., Rickerby, D., Mortensen, A., Jackson, P., Kyjovska, Z.O., Molhave, K., Jacobsen, N.R., Jensen, K.A., Yauk, C.L., Wallin, H., Halappanavar, S., Vogel, U., 2015. MWCNTs of different physicochemical properties cause similar inflammatory responses, but differences in transcriptional and histological markers of fibrosis in mouse lungs. Toxicol. Appl. Pharmacol. 284, 16–32.
Poulsen, S.S., Saber, A.T., Mortensen, A., Szarek, J., Wu, D., Williams, A., Andersen, O., Jacobsen, N.R., Yauk, C.L., Wallin, H., Halappanavar, S., Vogel, U., 2015. Changes in cholesterol homeostasis and acute phase response link pulmonary exposure to multi-walled carbon nanotubes to risk of cardiovascular disease. Toxicol. Appl. Pharmacol. 283, 210–222.
Sabella, S., Carney, R.P., Brunetti, V., Malvindi, M.A., Al-Juffali, N., Vecchio, G., Janes, S.M., Bakr, O.M., Cingolani, R., Stellacci, F., Pompa, P.P., 2014. A general mechanism for intracellular toxicity of metal-containing nanoparticles. Nanoscale 6, 7052–7061.
Saber, A.T., Koponen, I.K., Jensen, K.A., Jacobsen, N.R., Mikkelsen, L., Moller, P., Loft, S., Vogel, U., Wallin, H., 2012. Inflammatory and genotoxic effects of sanding dust generated from nanoparticle-containing paints and lacquers. Nanotoxicology 6, 776–788.
Saber, A.T., Jacobsen, N.R., Mortensen, A., Szarek, J., Jackson, P., Madsen, A.M., Jensen, K.A., Koponen, I.K., Brunborg, G., Gutzkow, K.B., Vogel, U., Wallin, H., 2012. Nanotitanium dioxide toxicity in mouse lung is reduced in sanding dust from paint. Part Fibre.Toxicol. 9, 4.
Sayes, C.M., Reed, K.L., Warheit, D.B., 2007. Assessing toxicity of fine and nanoparticles: comparing in vitro measurements to in vivo pulmonary toxicity profiles. Toxicol. Sci. 97, 163–180.
Stoeger, T., Reinhard, C., Takenaka, S., Schroeppel, A., Karg, E., Ritter, B., Heyder, J., Schulz, H., 2006. Instillation of six different ultrafine carbon particles indicates a surface area threshold dose for acute lung inflammation in mice. Environ. Health Perspect. 114, 328–333.
Vesterdal, L.K., Folkmann, J.K., Jacobsen, N.R., Sheykhzade, M., Wallin, H., Loft, S., Moller, P., 2010. Pulmonary exposure to carbon black nanoparticles and vascular effects. Part Fibre.Toxicol. 7, 33.
Warheit, D.B., Sayes, C.M., Reed, K.L., 2009. Nanoscale and fine zinc oxide particles: can in vitro assays accurately forecast lung hazards following inhalation exposures? Environ. Sci. Technol. 43, 7939–7945.
Wesselkamper, S.C., Chen, L.C., Kleeberger, S.R., Gordon, T., 2001. Genetic variability in the development of pulmonary tolerance to inhaled pollutants in inbred mice. Am. J. Physiol. Lung Cell Mol. Physiol. 281, L1200–L1209.
Xia, T., Zhao, Y., Sager, T., George, S., Pokhrel, S., Li, N., Schoenfeld, D., Meng, H., Lin, S., Wang, X., Wang, M., Ji, Z., Zink, J.I., Madler, L., Castranova, V., Lin, S., Nel, A.E., 2011. Decreased dissolution of ZnO by iron doping yields nanoparticles with reduced toxicity in the rodent lung and zebrafish embryos. ACS Nano 5, 1223–1235.